First Singlet (n,π^*) Excited State of Hydrogen-Bonded Complexes between Water and Pyrimidine

Zheng-Li Cai and Jeffrey R. Reimers*

School of Chemistry, The University of Sydney, NSW 2006, Australia

Received: April 19, 2004; In Final Form: November 25, 2004

Hydrogen bonds from water to excited-state formaldehyde and from water to excited-state pyridine have been shown to display novel motifs to traditional hydrogen bonds involving ground states, with, in particular for H_2O:pyridine, strong interactions involving the electron-rich π cloud dominating the (n,π^*) excited state. We investigate H_2O:pyrimidine and various dihydrated species and reveal another motif, one in which the hydrogen bonding can dramatically alter the electronic structure of the excited state. Such effects are rare for ground-state interactions for which hydrogen bonding usually acts to merely perturb the electronic structure of the participating molecules. It arises as the (n,π^*) excitation of isolated pyrimidine is delocalized over both nitrogens but asymmetric hydrogen bonding causes it to localize on just the noninteracting atom. As a result, the excited-state hydrogen bond in H_2O:pyrimidine is suprisingly very similar to the ground-state structure. These results lead to an improved understanding of the spectroscopy of pyrimidine in liquid water, and to the prediction that stable excited-state hydrogen bonds in H_2O:pyrimidine should be observable, despite failure of experiments to actually do so. They also provide a simple model for the intricate control over primary charge separation in photosynthesis exerted by hydrogen bonding, and for solvent-induced electron localization in symmetric mixed-valence complexes. All conclusions are based on strong parallels found between the results of calculations performed using density-functional theory (DFT) and time-dependent DFT (TDDFT), complete-active-space self-consistent-field (CASSCF) with second-order perturbation-theory correction (CASPT2) theory, and equation-of-motion coupled cluster (EOM-CCSD) theory, calculations that are verified through detailed comparison of computed properties with experimental data for both the isolated molecules and the ground-state hydrogen bond.

1. Introduction

Hydrogen bonding is very important in the molecular sciences as it plays a central role in the structure and function of all biological systems,[1−3] and hydrogen bonding involving azines/diazines and their derivatives is particularly significant. Although hydrogen bonding to molecules in their ground electronic state has been widely investigated by different spectroscopic[4−19] and theoretical[1,19−37] methods, much less is know about hydrogen bonding to molecules in excited states. Archetypal studies include the absorption and fluorescence studies that culminated in the work of Baba, Goodman, and Valenti,[4] supersonic molecular jet spectroscopy pioneered by Bernstein et al.,[8,9] and computations pioneered by Del Bene.[20−24] These studies consider the solvation of (n,π^*) excited states, states that are particularly revealing as the electronic transition removes one of the lone-pair electrons that directly participate in the hydrogen bonding. Here, we reveal a new motif in excited-state hydrogen bonding and use it to interpret experimental cluster and liquid spectroscopic data. The conclusions, based on a priori calculations, are shown to be robust with respect to variations between the best available computational methods, and consistent with a wide range of experimental data for simpler systems.

The basic concepts of excited-state hydrogen bonding were elucidated in 1966 by Baba, Goodman, and Valenti,[4] who studied the absorption and fluorescence spectra of pyridine and the diazines (pyridazine, pyrimidine, and pyrazine) in dilute solution in a variety of hydrogen-bonding and non-hydrogen-bonding solvents. They found that in hydrogen-bonding solvents the hydrogen bond formed between the solute in its ground electronic state and solvent molecules gives rise to a large blue shift in the (n,π^*) absorption transition but only small changes in the corresponding fluorescence spectrum. Dielectric solvation theories[29,38−40] express these solvent shifts as

$$\Delta U = -\frac{2\epsilon - 2}{2\epsilon + 1}\frac{1}{a^3}\mu_i\cdot(\mu_f - \mu_i) - \frac{n^2 - 1}{2n^2 + 1}\frac{1}{a^3}|\mu_f - \mu_i|^2 \quad (1)$$

where μ_i and μ_f are the dipole moment vectors of the initial and final states solvated outside a cavity of radius a by a material of dielectric constant ϵ and refractive index n. As the coefficient of the first term is much larger than that for the second, and as only the first term can give rise to a blue shift, Baba et al. qualitatively interpreted the experimental data as indicating a large dipole moment (ca. 3 D) from the ground state and a nearly zero dipole moment in the excited state. From this they concluded that the hydrogen bonding is broken in the (n,π^*) singlet excited state of pyridine and the diazines.

Their analysis appears quite valid for pyridine, but for the diazines it is incomplete as it does not properly address the issue of the localization/delocalization of the (n,π^*) excitation over the two nitrogen atoms. In the ground state, liquid-structure simulations indicate two hydrogen bonds are formed to the diazines.[26,27,30,41] In the excited state, if the excitation localizes onto one nitrogen atom, then this atom becomes analogous to

* Corresponding author. E-mail: reimers@chem.usyd.edu.au.

10.1021/jp048309i CCC: $30.25
Published on Web 02/05/2005

the nitrogen in pyridine and the other atom is unaffected. One would thus expect that the hydrogen bond to the unaffected nitrogen would remain intact and the other hydrogen bond would break. However, if the excitation is delocalized over both diazine nitrogen atoms, then each atom will have 1.5 electrons with which it may form hydrogen bonds to its environment, and it is not clear a priori whether hydrogen bonds are likely to form.[28−30,41]

Before the effects of through-bond interactions were known, strong interactions between nitrogen lone pairs were not expected and thus the excitation in pyrimidine and pyrazine (at least) were believed to be localized excitations,[41] even for uncomplexed pyrazine.[42] For pyrazine, however, the experimental results of Baba et al. do not support the idea of localized excitation, as this would guarantee a large change in dipole moment between the excited and ground states, and high-resolution spectroscopy clearly indicates that the (n,π*) excitation is delocalized in isolated pyrazine.[41] Similarly, for gas-phase pyrimidine, high-resolution spectroscopy clearly indicates that the excitation is delocalized in the excited state.[43]

Wanna, Menapace, and Bernstein[8,9] have studied the hydrogen-bonded and nonbonded van der Waals clusters, pyridazine, pyrazine, pyrimidine, and benzene (solutes), and C_nH_{2n+2}, NH_3, and H_2O (solvents) by the techniques of supersonic molecular jet spectroscopy and two-color time-of-flight mass spectroscopy. They did not observe pyridazine, pyrazine, or pyrimidine water clusters, however, and concluded that the excited states of these clusters must be dissociative. Nevertheless, stable excited states have actually been observed for a range of other azine complexes with hydrogen-bond donors,[6] indicating that a complete picture of the phenomenon has not yet been obtained. Currently, progress is hindered by the lack of detailed experimental information for these systems, and it is feasible that reliable theoretical calculations can provide new insight into the problem.

The electronic and geometrical structure of pyridine and the diazines in (n,π*) excited states in clusters and in aqueous solution have been simulated by Karelson and Zerner,[44,45] Zeng, Hush, and Reimers,[26,28−30,41,46] Gao and Byun,[32] and Almeida et al.[34] using combinations of semiempirical INDO/S[34,44,45] or AM1[32] methods with continuum solvation models,[44,45] QM/MM methods,[32] and analytical all-atom electrostatics methods.[26,29,30,41,46] Qualitatively, the nature of hydrogen bonding and calculated solvent shifts are found to be very sensitive to the details of the potential-energy surfaces and the method used to determine the effects of the hydrogen bonding on the electronic structure of the chromophore.

A focus of these studies has been understanding the process by which the observed blue shift of the (n,π*) band in solution arises; this shift is 0.33 ± 0.04 eV (2700 ± 300 cm^{-1}) for pyrimidine.[29] Karelson and Zerner[44,45] using INDO/S cluster calculations with a continuum description of the remaining solvent predicted a red shift for gap-phase complexes that was compensated by a huge blue shift following solvation. This result is not supported by any other calculation and is an artifact arising from their use of the unrealistic INDO/S optimized geometries for the clusters, geometries that embody a N−H hydrogen bond length of ca. 1.45 Å. Zeng, Reimers, and Hush[29] using a specifically parametrized molecular-mechanics force field to generate liquid configurations combined with a perturbative electrostatic treatment of the electronic effects of solvation predicted 0.17 eV (1380 cm^{-1}) shift for H_2O:pyrimidine[28] and 0.42 eV (3400 cm^{-1}) for the liquid,[29] Gao and Byun[32] using a AM1/TIP3P QM/MM method predicted 0.15 eV (1235 cm^{-1}) for H_2O:pyrimidine, 0.35 eV (2790 cm^{-1}) for the symmetric hydrogen-bonded complex H_2O:pyrimidine:H_2O, and 0.28 eV (2275 cm^{-1}) for the liquid, whereas Almeida et al.[34] using INDO/S energies evaluated at molecular-mechanics geometries predicted 0.28 eV (2230 cm^{-1}) for the liquid with only minor contributions coming from the directly hydrogen-bonded waters. Although these later methods share the same basic qualitative features, quantitatively they predict significantly different roles for the various contributions to the solvation effect. All methods rely on somewhat crudely estimated geometries, and all involve significant approximations to the evaluation of the transition energy at these geometries.

Further progress using computational means requires the application of high-level first-principles methods to the evaluation of structure and spectra. Though the hydrogen bonding between water and azines or diazines in their ground electronic states has been widely investigated using such methods,[1,11,14−17,30,31,37,41,47−54] only Del Bene[20−23] and ourselves[37] have similarly considered excited-state phenomena. Structural studies have only been performed for the HF:H_2CO complex by Del Bene at al.[24] and by ourselves[37] for H_2O:pyridine. Both of these studies reveal new motifs for hydrogen bonding that are not found for hydrogen bonds to ground-state molecules: for H_2CO this is a structure with hydrogen bond formation occurring at the oxygen in the C_s symmetry plane whereas for H_2O:pyridine a strong hydrogen bond is found from a water hydrogen to the electron-enhanced aromatic π cloud. As pyrimidine has two nitrogen atoms rather than the one of pyridine, it is not clear a priori if hydrogen bonding to its aromatic (n,π*) excited states will be similar to these or not.

Studies of azine−water clusters are of interest not only in terms of the mechanism of aqueous solvent shifts but also in their own right as these clusters can be made in molecular beam[8,9] and matrix-isolation[11] experiments. Our study[37] of H_2O:pyridine predicted that the additional energy provided to vertically excite the complex, the absorption "blue shift", significantly exceeded the dissociation energy of the complex in its (n,π*) excited state. As a result, H_2O:pyridine is expected to directly dissociate following (n,π*) excitation. Earlier, our more primitive calculations employing ab initio-optimized AMBER force fields[28,29] predicted that the blue shift for the diazines is actually less than that required for direct dissociation, suggesting that a stable excited-state complex could be obtained after excitation. These molecular-mechanics calculations were based on the assumption that the decocalized nature of the (n,π*) excitation for the diazines in the gas phase was retained after hydrogen-bond formation, and that the solvent acted merely to perturb this structure, a view not supported by the AM1-based QM/MM studies of Gao and Byun.[32] Again, we see that high-quality first-principles calculations are required to understand key properties of excited-state solvation.

Here we study the structures, energetics, and vibration frequencies of H_2O:pyrimidine and $2H_2O$:pyrimdine in their ground and first-excited (n,π*) states, using analogous first-principles computational methods for both the ground and excited states of these complexes. In particular, we use density functional theory (DFT) and time-dependent DFT[55−60] (TD-DFT) using the B3LYP[61] and BLYP[62,63] functionals, complete-active-space self-consistent-field (CASSCF[64]) with second-order perturbation-theory correction (CASPT2[65]), coupled-cluster theory (CCSD[66]), and equation-of-motion coupled-cluster (EOM-CCSD[67]) theory. These three methods are chosen as they embody quite different approaches to excited-state computations. Although each approach is capable of delivering the required degree of chemical accuracy necessary to study problems of

this type,[24,60] each has its particular, known, set of weaknesses, and we seek conclusions that are robust to computational methodology. This work follows from our recent comprehensive treatise of the excited-state manifolds of isolated pyrimidine[43] in which we considered in detail the energetics, structure, and vibrational motions of the molecule. However, due to the extensive computation requirements of excited-state hydrogen-bonding calculations, the ones performed herein are necessarily not of as high a quality as are those and other previous calculations involving ground-state hydrogen bonding. As the validity of the conclusions is in key parts based on the ability of the computational methods used to reproduce excited-state energy gaps, excited-state vibrational frequencies, and intermolecular interactions, particular care is taken to demonstrate the applicability of the methods.

2. Computational Details

TD-B3LYP calculations were performed by TURBOMOLE[68] using the "M3" integrating grid and the energy convergence criterion set to 10^{-10} au, with all derivatives evaluated numerically in internal coordinates using our own program. Computationally efficient auxiliary basis sets[69] were used for such calculations, facilitating excited-state geometry optimization. TD-BLYP geometry optimizations were performed for the excited states by using the CPMD[70] package. Direct DFT geometry optimizations and frequency calculations were performed for the ground-state with the aid of analytical derivatives using GAUSSIAN-98.[71] The CCSD[66] and EOM-CCSD[67] calculations were performed using analytical first derivatives by ACES−II.[72] CASSCF geometry optimizations were performed typically using DALTON,[73] but sometimes MOLCAS[74] or MOLPRO.[75] CASSCF harmonic frequency calculations were performed using the analytical derivatives available in the DALTON[73] package. Only single-point energy calculations were performed at the CASPT2 level, using the MOLCAS[74] package. In addition, one set of test CIS[76] geometry optimizations on the excited states were performed by using GAUSSIAN-98.

All calculations were performed using the 6-31+G* [77] basis set for pyrimidine and 6-31++G** [77] for water, 6-31+G*/6-31++G**. This is the smallest basis set combination that can provide a realistic description of both the nature of the excited states and the nature of the hydrogen bonds; larger basis sets will result in quantitative improvements in accuracy but are not currently feasible to apply. In our analogous study of H_2O:pyridine,[37] a range of basis sets was considered starting at aug-cc-pVDZ,[78] and the effects of basis set expansion beyond this level were seen to be relatively small, however. We find little degradation in performance in reducing the basis set from aug-cc-pVDZ to 6-31+G*/6-31++G**, but the computational efficiency is significantly improved. Previously we have used the cc-pVDZ[79] to assign the singlet and triplet excited-state manifolds gas-phase pyrimidine, and we also find little change upon reducing this to 6-31+G*.

Interaction energies (bonding energies), ΔE, for the complex AB are calculated using a problem-specific treatment of the basis set superposition error (BSSE) in addition to thermal and zero-point vibrational-energy (ZPE) corrections. These later corrections were obtained using the harmonic approximation to vibrational motion, with calculated frequencies scaled by factors[80] of 0.95 for CCSD and EOM-CCSD, 0.91 for CASSCF, 0.9614 for B3LYP, and 0.9945 for BLYP. As the hydrogen-bonding topologies are quite varied, appropriate treatment of BSSE is required to be able to properly compare the energies of different structures. For small basis sets, the BSSE is large and the counterpoise correction[81,82] is essential to apply, whereas for large basis sets the correction is dramatically reduced and becomes swamped by the extra binding that is facilitated by these larger basis sets so that its application enhances rather than reduces the associated errors.[83,84] The 6-31+G*/6-31++G** basis set is of intermediate size and hence it is not clear a priori whether the BSSE correction should be applied. We have studied this problem in detail for H_2O:pyridine[37] and find for the aug-cc-pVDZ basis set that the best results are obtained using a scaled BSSE correction

$$E_{\text{fract}} = E_{\text{raw}} + \lambda E_{\text{BSSE}} \tag{2}$$

where E_{BSSE} is the usual counterpoise correction, with λ optimized to be 0.51. As the 6-31+G*/6-31++G** basis set is for our practical purposes quite similar to aug-cc-pVDZ, we apply this same correction herein.

The CASSCF and CASPT2 calculations were performed using an active space[43] consisting of 18 electrons (includes all lone-pair and π electrons) distributed in 12 orbitals, $3a_1 + 4b_1 + 3b_2 + 2a_2$ in C_{2v} symmetry or $6a' + 6a''$ in C_s symmetry. This active space is not large enough so as to guarantee the continuity of the potential-energy surface of pyrimidine on displacement from its C_{2v} ground-state equilibrium geometry in all modes. Though continuous surfaces are highly desirable and intricacies concerning the design of active spaces for calculations on pyrimidine have been described elsewhere,[43] the CASSCF method is not quantitatively reliable for excited-state energy differences and hence continuity problems become of only minor significance; as is common practice, we use CASSCF only to optimize geometries, typically reporting only the more-reliable CASPT2 energies. The active space is not modified for use with hydrated molecules as the included pyrimidine orbitals lie well within the band gap of water and there is no direct involvement of water orbitals in the spectroscopic transitions studied.

3. Results and Discussion

Only a limited number of methods are available for excited-state geometry optimizations and frequency calculations, and computational feasibility significantly limits the size of the basis sets that may be applied. Before considering such calculations, we first examine the properties of the isolated pyrimidine and water monomers, and the properties of ground-state H_2O:pyrimidine, verifying that the methods we employ for the excited states in fact provide realistic descriptions of these well-studied systems. For reference, all ground and excited-state monomer and complex optimized geometries, vibration frequencies, and normal modes are provided in detail in Supporting Information.

3.1. Pyrimidine and Water Monomers. In Table 1 are shown the root-mean-square (RMS) differences between experimental[85−87] structural parameters and vibrational frequencies of water and of pyrimidine in their $^1A_1$ ground states (GS) and those calculated at the CASSCF, CCSD, B3LYP, and BLYP levels. Results from recent, possibly more extensive, calculations are also provided therein for comparison, whereas a more exhaustive and detailed survey is also available elsewhere.[43] In summary, all computed results are in good agreement with experiment.

Also shown in Table 1 are results for the first (n,π^*) S_1 state. For these, the CASPT2, CASSCF, EOM-CCSD, TD-B3LYP and TD-BLYP methods were used. The only available geometrical experimental results are the rotational constants, and these are reproduced adequately by our CASSCF and EOM-

TABLE 1: Comparison of Calculated and Experimental[a] Properties of the Water in Its Ground State and of Pyrimidine in Its Ground State (GS) and First (n,π^*) Excited State $^1B_1$

	RMS error in property						
	bond length/Å		bond angle/deg		frequency[b]/cm^{-1}		
		pyrimidine		pyrimidine		pyrimidine	
methods[b]	H_2O	GS	H_2O	GS	H_2O	GS	(n,π^*)
CASSCF	0.005	0.010	2.84	1.10	76	36	50
(EOM-)CCSD	0.005	0.008	0.96	1.07	39	16	60
(TD-)B3LYP	0.008	0.007	1.25	0.96	51	19	54
(TD-)BLYP	0.019	0.014	0.55	1.05	25	23	54

[a] From refs 85−87. [b] The vibrational frequencies are scaled by factors[80] of 0.91, 0.95, 0.9614, and 0.9945 for CASSCF, CCSD, B3LYP, and BLYP, respectively.

CCSD optimized geometries.[43] Eleven vibrational modes have been experimentally assigned[85] for S_1, and for these the RMS errors in the CASSCF and EOM-CCSD calculated frequencies are provided and are typically larger than those for the ground state. Additional errors arise because the most apparent modes in the spectra are often ones that are strongly vibronically active; vibronically active modes have significantly different frequencies in the ground and excited states, and the frequency shift is very sensitive to small errors in perceived excited-state energy gaps. Hydrogen bonding is subsequently shown to affect primarily the in-plane b_2 mode 6b, and hence it is critical that the computational methods describe it adequately. In the gas phase, this mode is observed[43] to decrease in frequency from 623 to 329 cm^{-1} upon excitation. Our previous calculations[43] using the cc-pVDZ basis set overestimate this effect, however, predicting 76i, 377i, and 312 cm^{-1} using EOM-CCSD, TD-B3LYP, and CASPT2, respectively; here, improved results are obtained using the 6-31+G* basis set of 167 and 212i cm^{-1} for EOM-CCSD and TD-B3LYP, with the lower accuracy CASSCF results predicting 402i cm^{-1}. It thus appears that for the discussion of the effects of excited-state hydrogen bonding on mode 6b, only the CASPT2 and EOM-CCSD methods are reliable.

Shown in Table 2 are calculated and observed vertical and adiabatic excitation energies for the S_1 (n,π^*) state of pyrimidine. Although it is usual to approximate the observed vertical excitation energy from the frequency of the absorption maximum, in quantitative studies it is important to obtain the best possible estimate of the average absorption energy and values are available for pyrimidine.[43] Also, the computed values need to be corrected for zero-point energy changes, but this is not feasible for all of the computational methods used. Our approach is therefore to determine "best estimated" zero-point energy changes using the computational methods for which vibrational frequencies can be evaluated. All computed zero-point energy changes are shown in Table 3, where our best-estimate values are defined. We apply this correction to the observed vertical excitation energies shown in Table 2 to obtain a direct comparison with the raw calculated values. Both the zero-point energy correction and the difference between the vertical excitation energy and the band-maximum energy are large compared with anticipated accuracy of modern computational methods; hence, in quantitative studies, their inclusion is essential.

As hydrogen bonding can induce significant geometrical distortions to azines in excited states,[37] it is essential that the computational methods used to study such phenomena provide proper treatment of electron−phonon coupling within a gas-phase chromophore. This in turn requires an adequate description of the entire singlet manifold of the molecule, and calculated excited-state vibration frequencies provide important information concerning the applicability of any method. Our results indicate that the electronic and vibrational properties of the $^1B_1$ lowest energy singlet excited state of pyrimidine obtained using TD-B3LYP, CASPT2, and EOM-CCSD with the 6-31+G* basis set agrees well with the available experimental data and with previous results[43] that we obtained using cc-pVDZ. These computational methods have been shown[43] to provide a comprehensive description of the singlet and triplet excited-state manifolds of pyrimidine and hence we anticipate that the present computational methods also correctly represent the excited-state manifold. They are thus expected to provide realistic descriptions of the effects of hydrogen bonding to the $^1B_1$ state. This is in contrast to alternate semiempirical methods that have been used to model hydrogen bonding to the $^1B_1$ state of pyrimidine as these place the low-lying $^1A_2$ (n,π^*) dark state of pyrimidine nearly degenerate with $^1B_1$,[34,44,45] introducing significant distortions to the shape of the potential-energy surface owing to the presence of a very low energy conical intersection.

TABLE 2: Calculated and Observed Vertical (E_v) and Adiabatic (E_0) Excitation Energies (eV) for the $^1B_1$ Lowest Singlet (n,π^*) Excited State of Pyrimidine

	E_v			E_0		
method	TD-B3LYP[a]	CASSCF[b]	EOM-CCSD[c]	TD-B3LYP[a]	CASSCF[b]	EOM-CCSD[c]
CASPT2	4.18	4.18	4.18	3.76	3.75	3.76
EOM-CCSD	4.71	4.70	4.72	4.27	4.26	4.28
TD-B3LYP	4.30	4.29	4.30	3.88	3.88	3.88
obs	4.20[d] (raw), 4.38[e] (after ZPE corr.)			3.85[f]		

[a] At the TD-B3LYP/6-31+G* optimized geometry. [b] At the CASSCF/6-31+G* optimized geometry. [c] At the EOM-CCSD/6-31+G* optimized geometry. [d] From ref 93. [e] After the correction for zero-point energy taken from Table 3; this value was 4.30 eV from previous calculations.[43] [f] From ref 85.

TABLE 3: Calculated Changes (eV) in Zero-Point Energy upon Complex Formation or Excitation for Pyrimidine (Py)−Water Clusters[a]

	Py + H_2O → H_2O:Py[b]		Py + 2H_2O → H_2O:H_2O:Py[c]		Py + 2H_2O → H_2O:Py:H_2O[d]		(n,π^*) excitation of			
method	GS	(n,π^*)	GS	(n,π^*)	GS	(n,π^*)	Py	H_2O:Py[b]	H_2O:H_2O:Py[c]	H_2O:Py:H_2O[d]
CASSCF	0.079	0.11	0.18	0.20	0.15	0.10	−0.19	−0.16	−0.17	−0.23
(TD-)B3LYP	0.068	0.09	0.16	0.17	0.14	0.01	−0.16	−0.15	−0.14	−0.29
(EOM-)CCSD	0.069	0.06					−0.18	−0.19		
best est.	0.072	0.09	0.17	0.19	0.15	0.06	−0.18	−0.17	−0.16	−0.26

[a] Ignoring intermolecular vibration of imaginary frequency. [b] For the C_s (planar) structure. [c] For the C_s (X_5) structure. [d] For the C_{2v} (S−E) structure.

TABLE 4: Calculated Interaction Energies[a] (ΔE, kcal mol^{-1}) after Fractional BSSE Corrections and Key Calculated Geometric Parameters (Bond Length in Å and Bond Angle in deg) for the Ground State (GS) and Lowest Singlet (n,π^*) Excited State of H_2O:Pyrimidine

			ΔE				bond lengths[d]				bond and torsion angles[d]						
state	structure	geometry	native	CC-SD	B3-LYP	CAS-PT2	N_1-H_{12}	N_3-H_{13}	N_1-O_{11}	N_3-O_{11}	$C_2-N_1C_6$	$C_2-N_3C_4$	$N_1H_{12}-O_{11}$	$N_3H_{13}-O_{11}$	$C_4N_1-H_{12}$	$C_6-N_3H_{13}$	$\tau N_1C_2-N_3C_4$
GS	C_s (planar)[a]	B3LYP	−5.91	−5.80	−5.91	−7.18	1.965		2.898		116.5	116.0	158.6		166.9		
		CASSCF		−4.46	−4.49	−5.74	2.147		3.037		116.9	116.6	155.9		164.4		
		CCSD	−6.12	−6.12	−5.81	−7.36	2.021		2.931		116.3	115.8	155.3		164.1		
		Expt.[b]					1.98		2.918				164.7				
(n,π^*)	C_s (planar)	TD-B3LYP	−4.91	−3.59	−4.91	−3.31	1.915		2.883		117.0	130.3	167.4		171.1		0
		CASSCF		−2.14	−1.67	0.55	2.146		3.081		118.0	128.2	168.2		167.4		0
		EOM-CCSD	−4.40	−4.40	−4.54	−3.14	2.029		2.961		118.1	129.8	160.3		165.6		0
		EOM-CCSD[c]	−2.58	−2.58	−2.91	−1.61	2.541		3.319		123.7	123.7	151.9		163.8		0
		TD-BLYP		−3.00	−4.93	−2.55	1.862		2.864		117.2	129.6	168.3		173.1		0
	C_1 (bif)	TD-BLYP		−1.98	−2.60	−1.62	2.704	3.611	3.628	4.030	117.8	129.1	154.4	108.1	88.2	69.8	3.6
	C_1 (top)	TD-BLYP		−2.81	−3.31	−2.00	2.187	4.261	3.171	4.532	118.2	129.5	167.0	99.6	114.2	61.0	2.7
	C_s (top)	TD-BLYP		−0.11	−1.69	2.14	3.199	3.199	3.932	3.932	125.4	125.3	131.0	130.9	87.7	87.3	10.2

[a] Previous calculations include −4.45 kcal mol^{-1} using HF/6-31G**,[19] −5.12 kcal mol^{-1} using MP2/6-31G**,[19] −6.89 kcal mol^{-1} using MP2/6-31++G**;[11] and −4.7 kcal mol^{-1} using QM/MM.[32] [b] From ref 19. [c] Pyrimidine constrained to C_{2v} symmetry without optimization with H_2O optimized, the total energy being only 533 cm^{-1} higher than that for the fully optimized in-planar distorted H_2O:pyrimidine. [d] Atom numbers are defined in Figure 1.

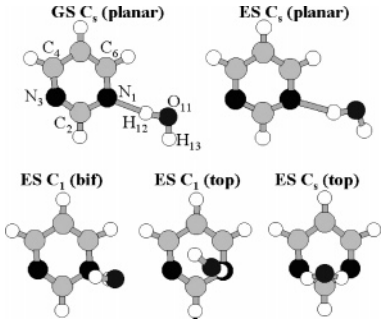

Figure 1. Hydrogen-bonded structures for the ground (GS) and (n,π^*) excited state (ES) of H_2O:pyrimidine calculated using (TD-)B3LYP with the 6-31+G* basis set for pyrimidine and 6-31++G** for water.

3.2. H_2O:pyrimidine Complex. *3.2.1. Ground State.* This hydrogen-bonded complex has been the subject of many investigations,[1,6,11,18,19,21,25−35,88] and its basic structure and energetics are known. As our interest is in vibrational analyses and excited states, we employ more approximate methods than have otherwise been used. Results are provided in Table 4 (key structural and energetic information), Figure 1 (structures), and the Supporting Information (complete listing of structures, energies, vibrational frequencies, and normal modes, with key normal-mode displacements and Duschinsky matrices). The convention used for the atom names is indicated in the figure. Initially we considered several possible structures for the H_2O:pyrimidine complex selected by analogy to those found relevant for H_2O:pyridine:[37] two bifurcated structures with C_{2v} symmetry and the water molecule located either planar or perpendicular to the pyrimidine, named C_{2v}(planar) and C_{2v}(perp), respectively, two analogous single hydrogen-bonded structures with C_s symmetry, named C_s(planar) and C_s(perp), and one which is a modification of the C_s(perp) structure having C_1 symmetry. Only the planar structure with C_s symmetry, the one with the lowest calculated bonding energy, is depicted in Figure 1; note too that as the optimized B3LYP, CASSCF, and CCSD structures all appear quite similar, only one respective structure, that from B3LYP, is actually presented.

In more detail, our calculated results for the cluster structure and energetics are shown in Table 4, together with previous theoretical and available experimental results. The calculated bonding energies from the reliable CCSD and B3LYP methods are in the range 5.9−6.1 kcal mol^{-1}. It is very common in excited-state calculations to use practicable CASSCF calculations to optimize geometries and higher methods such as CASPT2 to determine relaible energies at these geometries. The results shown in Table 4 indicate that this is not an appropriate method for states involving hydrogen bonding, however, as the CCSD and B3LYP transition energies at the CASSCF geometries differ significantly from the fully optimized ones.

Consistent with the general notion that hydrogen bonding causes only small perturbations to the electronic structures of the participating molecules, the geometrical properties shown in Table 4 indicate that only small structural changes are predicted for pyrimidine on hydrogen bonding; these results are in stark contrast to forthcoming ones for excited-state hydrogen bonding, however. In the Supporting Information, a detailed comparison is provided between observed and calculated vibrational frequencies for the complex. However, one of the most important experimentally accessible signatures of the hydrogen bonding is the shift of the OH vibration frequency, and it is essential that the computational methods be demonstrated to properly reproduce this feature. Matrix isolation studies[11] reveal a red shift of 201 cm^{-1} for this mode, whereas the B3LYP and CCSD methods predict 212 and 116 cm^{-1}, respectively. Although this CCSD result is only qualitatively reliable, basis set expansion should produce quantitative accuracy. Most important, it is clear that these computational methods do not overestimate the effects of hydrogen bonding and hence they can be considered to be qualitatively reliable in related circumstances for which large changes are actually predicted.

3.2.2. Lowest (n,π^*) Excited State. Four different structures for the (n,π^*) state of H_2O:pyrimidine were optimized at the CASSCF, TD-B3LYP, and EOM-CCSD levels, and the results are shown in Table 5 (adiabatic and vertical excitation energies), Table 4 (structures and fractional-BSSE-corrected interaction energies), Figure 1 (structures), and the Supporting Information (complete description, including analysis of geometric and frequency changes by mode). One of these structures, named C_s(planar), is analogous to the minimum-energy structure reported for the ground state; two named C_1(top) and C_s(top) have the water above the pyrimidyl ring interacting simultaneously with the π cloud and the nitrogen atoms, with the C_s(top) structure maintaining the equivalence of the two nitrogen atoms, and another named C_1(bif) in which both water hydrogens interact with the same nitrogen from a position above the

TABLE 5: Calculated Vertical Excitation Energies (E_v), as Well as Fractional BSSE-Corrected Origin Excitation Energies (E_{00}) and Predissociation Energies (E_{Pre}), for H_2O:Pyrimdine and $2H_2O$:Pyrimdine Excited States, after Correction for Errors in the Calculations of Isolated Pyrimidine (All in eV)

method	geometry	$E_v - E_v$(Py)[a]	E_v	E_{dir}	E_{pre}	E_{00}	$E_{00} - E_{00}$(Py)
		Pyrimidine Monomer[e]					
observed		[0]	4.20[e]			3.85[f]	[0]
		H_2O:pyrimidine					
TD-B3LYP	TD-B3LYP	0.10	4.30	4.38	4.03	3.90	0.05
	EOM-CCSD	0.11	4.31	4.38	4.03	3.91	0.06
EOM-CCSD	TD-B3LYP	0.12	4.32	4.38	4.03	3.96	0.11
	EOM-CCSD	0.11	4.31	4.39	4.04	3.92	0.07
CASPT2	TD-B3LYP	0.25	4.45	4.44	4.09	4.03	0.18
	EOM-CCSD	0.24	4.44	4.45	4.10	4.04	0.19
QM/MM[b]	QM/MM[b]	0.15					
INDO/S[c]	INDO/S[c]	−0.15					
classical[d]	AMBER[d]	0.17					
		H_2O:H_2O:Pyrimidine					
TD-B3LYP	TD-B3LYP	0.15	4.35	4.65	4.30	3.91	0.06
	EOM-CCSD	0.16	4.36	4.70	4.35	3.96	0.11
EOM-CCSD	TD-B3LYP	0.17	4.37	4.75	4.39	4.00	0.15
	EOM-CCSD	0.16	4.36	4.71	4.36	3.97	0.12
CASPT2	TD-B3LYP	0.32	4.52	4.79	4.44	4.05	0.20
	EOM-CCSD	0.31	4.51	4.83	4.48	4.09	0.24
		H_2O:Pyrimidine:H_2O					
TD-B3LYP	TD-B3LYP	0.16	4.36	4.48	4.13	3.96	0.11
	EOM-CCSD	0.17	4.37	4.49	4.14	3.97	0.12
EOM-CCSD	TD-B3LYP	0.19	4.39	4.49	4.14	3.97	0.12
	EOM-CCSD	0.19	4.39	4.45	4.10	3.93	0.09
CASPT2	TD-B3LYP	0.19	4.39	4.49	4.14	3.97	0.12
	EOM-CCSD	0.19	4.39	4.45	4.10	3.93	0.09
QM/MM[b]	QM/MM[b]	0.35					
INDO/S[c]	INDO/S[c]	−0.25					
classical[d]	AMBER[d]	0.25					

[a] 0.33± 0.04 eV obtained from analysis of experimental data in aqueous solution (see refs 28 and 29 for more details). [b] From QM/MM simulations,[32] 0.28 ± 0.01 eV in aqueous solution. [c] From semiempirical calculations,[44,45] 0.32 eV in aqueous solution or 0.28 ± 0.01 eV from more recent results.[34] [d] From classical electrostatics simulations,[28,29] 0.42 eV in aqueous solution. [e] From ref 93. [f] From ref 85.

pyrimidyl plane. In most structures, the pyrimidyl ring remains very close to planar, with an indication of nonplanarity given by the torsional angle $\tau N_1C_2N_3C_4$ in Table 4; the largest deviation is 10.2° for the C_s(top) structure. These structures are in stark contrast to the ones found for H_2O:pyridine for which the excited-state equilibrium hydrogen-bonded structure undergoes a large boat distortion due to modulation of the strong vibronic coupling between the $^1B_1$ (n,π^*) state of interest and a nearby $^1A_1$ (π,π^*) state.

The fractional-BSSE-corrected interaction energies ΔE evaluated at these geometries using the CASPT2, TD-B3LYP, and EOM-CCSD methods are given in Table 4. These results indicate that the planar C_s structure is more stable than the others, although the energy difference from the C_1(top) structure is variable, ranging from 0.2 kcal mol^{-1} by EOM-CCSD to 0.6 kcal mol^{-1} from CASPT2 to 1.6 kcal mol^{-1} from TD-B3LYP. TD-B3LYP and EOM-CCSD predict that the binding energy of the planar C_s configuration is quite large, $-\Delta E = 4.9$ and 4.4 kcal mol^{-1}, respectively, only 1.0 and 1.7 kcal mol^{-1} less strongly bound than the analogous ground-state complexes, whereas CASPT2 predicts weaker bonding of ca. $-\Delta E = 3.3$ kcal mol^{-1}. Unfortunately, optimized excited-state coordinates could only be completed using the TD-BLYP method for all structures, and hence it is possible that these most significant results are not robust to variation in the computation scheme used. As an additional test, we performed CIS geometry optimizations for all structures starting at the TD-BLYP optimized coordinates. *All* of these optimizations led to the C_s-(planar) configuration, supporting the notion that it is the most important excited-state hydrogen-bonded configuration.

TABLE 6: In-Plane Distortion of Pyrimidine Caused by the Hydrogen Bonding of Water in Structure C_s (X_5) to the Lowest Singlet (n,π^*) Excited State, Analyzed in Terms of the Dominant Distortion in Mode 6b of the Excited State[a]

method	ν_{6b}/cm^{-1}	δ_{6b}	λ_{6b}/eV	λ_{tot}/eV (harmonic)	λ_{tot}/eV (exact)
TD-B3LYP	212*i*	0.98	−0.013	0.04	0.001
CASSCF	402*i*	1.39	−0.048	−0.033	
EOM-CCSD	167	0.28	0.008	0.02	0.018

[a] ν is the calculated vibration frequency, δ is the dimensionless displacement in terms of the calculated normal coordinates of pyrimidine, $\lambda_{6b} = h\nu_{6b}\delta_{6b}^2/2$ is the component reorganization energy, and λ_{tot} is the total reorganization energy evaluated either approximately from the sum of the projected harmonic components or exactly from the calculated distortion energy of the pyrimidine in H_2O:pyrimidine.

For H_2O:pyridine,[37] analogous in-plane conventional hydrogen-bonded structures and above-ring structures were also predicted, but by far the lowest energy structure was an above-ring one similar to the C_1(top) structure in which the water hydrogen-bonded to the aromatic π cloud but the pyridine also buckled severely, losing its planarity. The stability of the planar C_s structure for H_2O:pyrimidine is thus a new feature that can be understood in terms of localization of the (n,π^*) excitation on the non-hydrogen-bonded nitrogen of the diazine. The calculated CNC bond angles at the EOM-CCSD level of 118° (bonded nitrogen) and 130° (nonbonded nitrogen) for H_2O:pyrimidine reflect this localization. For isolated pyrimidine,[43] the (n,π^*) state retains C_{2v} symmetry and the analogous calculated bond angles are both 123°, indicating that in this case the excitation remains delocalized. Hence the effect of hydrogen bonding on the (n,π^*) excited state of pyrimidine cannot be treated as merely providing a perturbation to the gas-phase electronic structure of the chromophore; rather, it changes its qualitative nature, affecting all chemical and spectroscopic properties of the molecule. Note that the C_s(top) structure is optimized subject to the constraint of C_s symmetry and embodies full delocalization of the (n,π^*) excitation. Its energy is predicted to be 1.6−2.7 kcal mol^{-1} higher than the analogous excitation-localized structure C_1(top).

The in-plane distortion to pyrimidine induced by hydrogen bonding can be analyzed not only in terms of changes in bond lengths and angles but also in terms of displacements in the normal modes of pyrimidine. Full results are presented in Supporting Information, and the overall properties and those with respect to displacement in the most sensitive mode,[85] 6b, are described in Table 6. Experimentally,[43] in the lowest (n,π^*) state of pyrimidine this mode is observed to be quite harmonic with a vibration frequency of 329 cm^{-1}. In our previous calculations with the cc-pVDZ basis set, only CASPT2 predicted a scenario in qualitative agreement with this, the calculated frequency being 312 cm^{-1}, whereas TD-B3LYP and EOM-CCSD predicted double-minimum potentials with barrier frequencies of 377i and 76i cm^{-1}, respectively. The results of 212i and 167 cm^{-1}, respectively, shown in Table 6 were obtained using the 6-31+G* basis and depict significant improvement on the previous cc-pVDZ ones. The (n,π^*) localization for H_2O:pyrimidine predicted by TD-B3LYP may arise purely from the inability of the method to correctly describe pyrimidine itself, whereas EOM-CCSD may predict this result only because it underestimates ν_{6b} and hence the required distortion energy. To

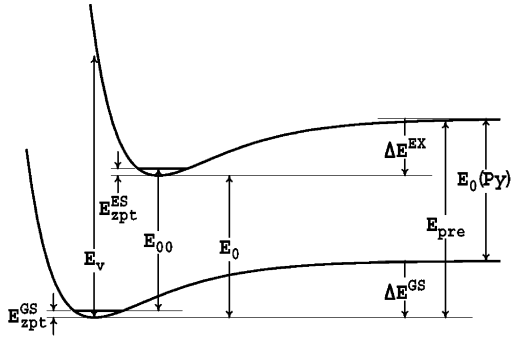

Figure 2. Schematic potential-energy surfaces for the ground state (GS) and excited state (ES) of H_2O:pyrimidine as a function of some dissociative intermolecular coordinate, inciding the adiabatic excitation energy of pyrimidine monomer, E_0(Py), the vertical, adiabatic, and origin transition energies of complex, E_v, E_0, and E_{00}, respectively, the zero-point energies E_{ZPT}^{GS} and E_{ZPT}^{ES}, and the hydrogen-bond interaction energies ΔE^{GS} and ΔE^{ES}.

investigate this possibility, Table 6 shows the projection of the distortion away from C_{2v} symmetry induced by hydrogen bonding projected onto the normal coordinate of mode 6b, the reorganization energy λ_{6b} associated with this projection, the total reorganization energy evaluated using all normal modes, and the total reorganization energy evaluated directly as the energy required to distort gas-phase excited-state pyrimidine from its equilibrium geometry to that predicted for the complex. Good agreement of these two quantities is found only from the EOM-CCSD calculations as the other methods depict quartic rather than harmonic surfaces. The effects caused by underestimation of the vibration frequency of mode 6b may be estimated simply by rescaling λ_{6b} to $0.007 \times (329/167)^2 = 0.027$ eV. Hence, the predicted distortion would cost 0.020 eV = 0.46 kcal mol^{-1} more energy. As this amount is small compared to the hydrogen-bond energy and the energy differences to alternate structures, improved calculations should continue to predict spontaneous localization of the (n,π*) state on hydrogen bonding.

To provide data relevant to the possible observation of stable (n,π*) excited states of H_2O:pyrimidine in a following photoexcitation in a molecular beam, Table 5 shows a variety of deduced energetic parameters. The quantities involved are sketched in Figure 2 and include the appropriate zero-point energies E_{zpt}, interaction energies ΔE, complex vertical (E_v), adiabatic (E_0), and origin (E_{00}) transition energies, as well as the adiabatic transition energy for isolated pyrimidine, E_0(Py). This figure is sketched along an idealized coordinate that starts from the linear hydrogen-bonded structure of the ground state and progresses to molecular dissociation. The excited-state minimum is indeed accessible without barrier from the ground-state geometry, as indicated qualitatively in the figure. In addition, two other energies provide indicators of the types of dynamics likely on the excited-state potential-energy surface. These are the predissociation energy

$$E_{pre} = E_{00}(\mathrm{Py}) - \Delta E^{GS} - \Delta E_{zpt}^{GS} \qquad (3)$$

which specifies the minimum energy for optical excitation that could possibly lead to dissociation of the complex in the excited state, where E_{00}(Py) is the 0-0 transition energy of gas-phase pyrimidine and ΔE_{ZPT}^{GS} is the change in zero-point energy due to complex formation in its ground electronic state. For dissociation to occur at this excitation energy, all energy imparted into vibrational motions of the pyrimidine molecule must be converted to translational energy of the fragments, however. This energy is also indicated in Figure 2; the second energy is that required for direct dissociation *without* the need for energy transfer from the excited vibrations of pyrimidine. As this energy is dependent on the specific vibronic level of the complex which is excited, we consider only excitation at the band center and express the band-center direct dissociation energy as

$$E_{dir} = E_v(\mathrm{Py}) - \Delta E^{GS} - \Delta E_{zpt}^{GS} \qquad (4)$$

where E_v(Py) is the vertical excitation energy of gas-phase pyrimidine.

Table 5 provides best estimate predictions of the actual molecular properties by correcting the computed transition energies for the known errors of each particular method in predicting the transition energies of isolated pyrimidine. In this fashion, E_v and E_{00} for the complex are evaluated by adding to the calculated value of $E_v - E_v$(Py) the observed value for E_v-(Py), etc.

For the (n,π*) excited state, the EOM-CCSD and TD-B3LYP calculations indicate that the predissociation energy E_{pre} of the complex is in excess of the 0−0 energy E_{00} by ca. 0.1 eV and hence predict that bound excited-state complexes can be found. However, the vertical excitation energy E_v from the ground state is predicted to exceed the dissociation energy by ca. 0.3 eV and hence careful control of the excitation energy is required to prevent predissociation. Further, the vertical excitation energy is predicted to be very close to the direct dissociation energy E_{dir}. Hence energy transfer from intramolecular to intermolecular motions is not required for the vertically excited complex to predissociate and so the dissociation process is expected to be very rapid indeed.

As a means to help in the interpretation of the observed spectroscopic data for pyrimidine in solution, the calculated solvent shifts $E_v - E_v$(Py) are given in Table 5 and are of order 0.10−0.11 eV (800−900 cm^{-1}), as evaluated using TD-B3LYP and EOM-CCSD and 0.22−0.25 eV (1800−2000 cm^{-1}) from CASPT2. Qualitatively, these results are similar to those from the pioneering ab initio studies of Del Bene.[21] Quantitatively, the EOM-CCSD results are expected to be more reliable than the CASPT2 ones, and the good agreement of the EOM-CCSD and TD-B3LYP results is encouraging. The best-estimate calculated solvent shift of 0.10−0.11 eV is considerably less than the value of 0.17 eV predicted by Zeng, Reimers, and Hush[29] using a perturbative molecular-mechanics model based on the assumption that no hydrogen-bond-induced change to the qualitative nature of the electronic structure of pyrimidine occurs, and slightly less than the AM1/TIP3P QM/MM result of Gao and Byun[32] of 0.15 eV; they are qualitatively different from the INDO/S result of −0.15 cm^{-1} from Karelson and Zerner,[44,45] however.

As shown in Figure 2, the blue shift of the vertical excitation energy arises owing to the reduced hydrogen-bond strength in the excited state; this effect also gives rise to an expected red shift of fluorescence band maximum. Our calculated shift in the vertical emission energy of H_2O:pyridine is −0.07 eV (−560 cm^{-1}), only ca. 300 cm^{-1} less in magnitude that the calculated vertical absorption shift. These quantities are similar as the excitation localizes on the non-hydrogen-bonded nitrogen and hence large solvent effects do not arise. In liquid solution,[4,29] the observed emission shift is of the same magnitude as it is for H_2O:pyrimidine, −0.07 eV (−600 cm^{-1}), whereas the absorption shift expands dramatically to 0.33 ± 0.04 eV (2700 ± 300 cm^{-1}). These results are consistent with the original

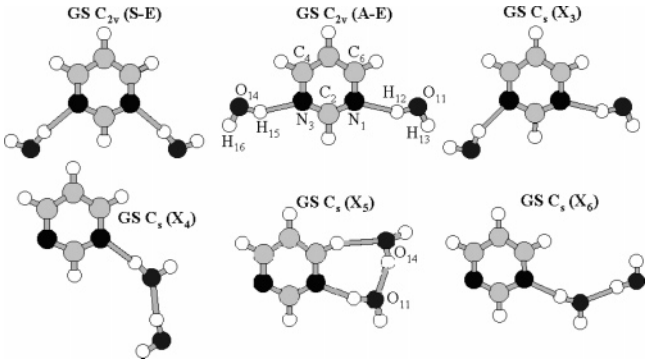

Figure 3. Optimized hydrogen-bonded structures for the ground state (GS) of $2H_2O$:pyrimidine.

TABLE 7: Calculated Interaction Energies ΔE (kcal mol^{-1}) after Fractional BSSE Corrections, for Two Water Molecules Hydrogen-Bonded to the Ground State of Pyrimidine[a]

structure	B3LYP	CCSD	CASPT2
C_{2v}(S−E)	−10.09	−9.86	−12.06
C_{2v}(A−E)	−11.45	−11.47	−13.74
X_3	−10.94	−11.08	−13.61
X_4	−12.00	−11.61	−14.19
X_5	−15.14	−14.82	−17.64
X_6	−12.28	−11.82	−14.53
max. BSSE	1.04	2.74	2.81
av BSSE	0.77	2.16	2.10

[a] At the B3LYP/6-31+G*/6-31++G** optimized geometry.

conclusions of Baba, Goodman, and Valenti[4] based on the assumption that the excitation localized on one nitrogen only, meaning that further solvation does not affect this nitrogen in the excited state whereas both nitrogen atoms are equally solvated in the ground state.

3.3. $2H_2O$:pyrimidine Complexes. *3.3.1. Ground State.* On the basis of the results of previous studies,[28,29] six possible structures for the ground state of $2H_2O$:pyrimidine have been investigated, and the relevant optimized structures are shown in Figure 3. All geometry optimizations were performed using B3LYP. The interaction energies for the two waters to the ground state of pyrimidine evaluated using B3LYP, CCSD, and CASPT2 are shown in Table 7. The most stable structure is predicted to be X_5, a planar structure of C_s symmetry. Compared to the structure of H_2O:pyrimidine, this one has the additional water bonded to the first water, with the two water molecules lying in the pyrimidyl plane forming a ring structure involving an apparent weak C−H linkage; it is described more informatively as H_2O:H_2O:pyrimidine. Symmetric structures are also found that have one water molecule hydrogen-bonded to each nitrogen of which the lowest energy one is C_{2v} (A−E); it is described more informatively as H_2O:pyrimidine:H_2O. The symmetric structures are 4−5 kcal mol^{-1} less stable than the asymmetric one X_5. Addition of the first water to pyrimidine released ca. 6 kcal mol^{-1} energy, addition of a second water as H_2O:H_2O:pyrimidine releases a further ca. 9 kcal mol^{-1}, but addition of a second water as H_2O:pyrimidine:H_2O releases only an additional 4−5 kcal mol^{-1} owing to unfavorable pyrimidine polarization.

A more detailed analysis of the calculated interaction energies, as well as some key geometric parameters, are provided in Table 8 for structures of type H_2O:H_2O:pyrimidine and H_2O:pyrimidine:H_2O. For H_2O:H_2O:pyrimidine, the computational methods predict CNC bond angles of 115.9° and 116.8°, very close to the value of 116.5° for H_2O:pyrimidine from Table 4 and the value of 116.7° for H_2O:pyrimidine:H_2O. Hence we see that ground-state hydrogen bonding does not significantly perturb the molecular structure of pyrimidine. Little variation is also found between the calculated N- -H hydrogen-bond lengths, again indicating that, despite the above-mentioned changes in the electrostatic component of the interaction energy, ground-state hydrogen bonding to the two nitrogen atoms is perturbative and nearly additive in nature.

In Supporting Information, a detailed comparison is also provided for the calculated vibrational frequencies of the X_5 and S−E complexes. The most interesting feature of these data is that for X_5 the calculated B3LYP red shift of 185 cm^{-1} in the azine hydrogen-bonded O−H stretch frequency is less than the value of 212 cm^{-1} reported for H_2O:pyrimidine where an enhanced red shift would naively be expected. The calculated frequency shifts are generally very similar to those for H_2O:pyrimdine.

3.2.2. Lowest (n,π) Excited State of H_2O:H_2O:Pyrimidine and H_2O:Pyrimidine:H_2O.* Structures for the lowest energy (n,π*) excited state of the X_5 and S−E structures of $2H_2O$:pyrimidine were optimized at the CASSCF, TD-B3LYP, and EOM-CCSD levels starting at the respective ground-state geometries, and the results are shown in Table 8 (structures and fractional-BSSE-corrected interaction energies), Table 5 (vertical and adiabatic excitation energies, predissociation and direct dissociation energies), Table 3 (zero-point energies), and the Supporting Information (complete description of structures and vibration frequencies, including an analysis of frequency

TABLE 8: Calculated Interaction Energies ΔE (kcal mol^{-1}) after Fractional BSSE Corrections and Key Calculated Geometric Parameters (Bond Lengths in Å and Bond Angles in deg) for the Ground State (GS) and Lowest Singlet (n,π*) Excited State of $2H_2O$:Pyrimdine

			ΔE				bond lengths[b]					bond angles[b]				
state	structure	geometry	native	CCSD	B3-LYP	CAS-PT2	N_1−O_{11}	N_1−O_{14}	N_1−H_{12}	N_1−H_{15}	O_{11}−H_{15}	C_2N_1-C_6	C_2N_3-C_4	N_1H_{12}-O_{11}	N_1O_{11}-H_{15}	$O_{11}N_1$-O_{14}
GS	C_s (X_5)[a]	B3LYP	−15.14	−14.82	−15.14	−17.64	2.833	3.767	1.879	3.452	1.857	116.8	115.9	162.0	101.2	47.2
		CASSCF		−13.23	−12.70	−15.36	3.003	3.952	2.082	3.644	1.998	117.1	116.5	162.1	102.0	46.8
		CCSD	−15.13	−15.13	−15.05	−17.61	2.906	3.850	1.968	3.546	1.920	116.5	115.7	160.5	100.6	47.1
	C_{2v} (SE)	B3LYP	−10.09	−9.86	−10.09	−12.06	2.954	4.949	1.994	4.115	6.068	116.7	116.7	167.3	37.1	110.9
		CASSCF		−9.39	−7.78	−9.64	3.106	5.072	2.171	4.252	6.256	117.0	117.0	168.4	37.8	109.7
		CCSD	−10.04	−10.04	−9.93	−11.97	2.998	4.946	2.050	4.946	5.993	116.3	116.3	165.2	39.5	106.2
(n,π*)	C_s (X_5)	TD-B3LYP	−13.43	−11.94	−13.43	−13.42	2.825	3.758	1.867	3.445	1.865	117.6	130.8	162.6	101.1	47.6
		CASSCF		−9.78	−8.73	−8.23	2.998	4.091	2.071	3.705	2.003	117.9	128.3	164	107.4	45.6
		EOM-CCSD	−12.74	−12.74	−12.89	−12.61	2.874	3.988	1.927	3.618	1.939	117.5	130.5	162.8	105.5	45.8
	C_{2v} (SE)	TD-B3LYP	−5.75	−5.32	−5.75	−7.45	2.953	4.789	2.006	3.989	5.843	124.2	124.2	163.3	41.3	106.5
		CASSCF		−4.89	−3.52	−6.63	3.188	4.747	2.380	4.209	5.520	124.4	124.4	143.3	49.4	85.6
		EOM-CCSD	−6.84	−6.84	−5.54	−8.70	3.010	4.518	2.221	4.055	5.154	124.4	124.4	138.1	51.8	81.1

[a] −9.0 kcal mol^{-1} evaluated using a QM/MM method.[32] [b] Atom numbers are defined in Figure 3.

changes by mode). No qualitative changes to the structures arose during this process, with the final structures closely resembling the starting ones shown previously in Figure 3.

The calculated EOM-CCSD and TD-B3LYP bonding energies for H_2O:H_2O:pyrimidine after corrections are 12.7 and 13.4 kcal mol^{-1}, respectively, 2.4 and 1.7 kcal mol^{-1} less than those predicted for the analogous ground-state structures. These destabilizations of the excited-state hydrogen bonding exceed those of 1.7 and 1.0 kcal mol^{-1}, respectively, noted earlier for H_2O:pyrimidine; they become directly manifest through a solvation-enhanced red shift, an effect later discussed in depth. The calculated CNC bond angles of 118° and 131° are very similar to those for H_2O:pyrimidine and indicate that the (n,π^*) excitation remains localized, as one would expect given that the second water acts to increase the asymmetry.

In contrast, the optimized structure for H_2O:pyrimidine:H_2O has equivalent CNC bond angles, whereas the B3LYP normal-mode frequencies from Supporting Information indicate that it is stable with respect to asymmetric distortions. Its electronic structure is thus akin to that for isolated pyrimidine. This result again indicates that the electronic structure of pyrimidine in its first (n,π^*) excited state is dramatically altered by hydrogen bonding and is now seen to be very sensitive to variations in the hydrogen-bonding topology.

From Table 8 it costs ca. 2 kcal mol^{-1} more in energy to excite H_2O:pyrimidine:H_2O than it does to excite H_2O:H_2O:pyrimidine, and this contributes to an enhanced blue shift for this complex. Most interesting, however, is the prediction that the total binding for H_2O:pyrimidine:H_2O in its (n,π^*) excited state is ca. 6 kcal mol^{-1}, very similar to the binding for ground-state H_2O:pyrimidine. It requires 1−2 kcal mol^{-1} of energy to dissociate the symmetric ternary complex

$$H_2O\text{:pyrimidine}^*\text{:}H_2O \rightarrow H_2O\text{:pyrimidine}^* + H_2O$$

however, and hence this quantity can be considered to be the excited-state second hydrogen-bond energy.

The feasibility of detection of excited-state hydrogen-bonded clusters is examined through the calculated values of the band origins, vertical excitation energies, predissociation energies, and direct dissociation energies given in Table 5 for H_2O:H_2O:pyrimidine and H_2O:pyrimidine:H_2O. Analogous to the results described earlier for H_2O:pyrimidine, the symmetrical doubly bonded species is predicted to have a predissociation energy that is only ca. 0.15 eV above E_{00} and hence will either be rather difficult to observe or may in reality be completely unbound. However, double asymmetric solvation stabilizes the excited state so that for H_2O:H_2O:pyrimidine the predissociation energies E_{pre} is predicted to be in excess of E_{00} by ca. 0.4 eV. Further, for this species the vertical excitation energy is predicted to be below the direct dissociation energy E_{dir} by ca. 0.35 eV, requiring that energy transfer from intramolecular to intermolecular motions must occur before the vertically excited complex predissociates. Hence optical excitation of this species is expected to provide stable and long-lived excited-state complexes in high yield. The lifetime of the stable excited-state complexes will of course be limited by the rate of internal energy transfer to the S_0 ground state of the pyrimidine molecule as this process makes the entire absorbed energy available to chemical processes.

The EOM-CCSD and TD-B3LYP calculated solvent shifts $E_v - E_v$(Py) given in Table 5 are of order 0.11 eV (900 cm^{-1}) for single hydration in H_2O:pyrimidine, 0.16 eV (1300 cm^{-1}) for asymmetric double hydration in H_2O:H_2O:pyrimidine, and 0.18 eV (1500 cm^{-1}) for double symmetric hydration in H_2O:pyrimidine:H_2O. These shifts are qualitatively similar to those predicted using classical electrostatics simulations based on geometries optimized using a molecular-state specific AMBER force field:[29,46] 0.17 eV for monohydration, 0.25 eV for inner-shell hydration, ca. 0.38 eV including the second hydration shell, and 0.42 eV including the third shell. Quantitatively, the ab initio evaluated cluster red shifts are all of order 60% of these from the electrostatic simulations, however, an effect in part owing to the tendency of the excitation to localize on just one nitrogen. This effect was not included in the previous calculations as they had explicitly assumed that the electronic structure of the hydrated chromophore could be expressed perturbatively in terms of that of the gas-phase species. On the basis of the close analogy found between the results of our current first principles methods and these simulations, it is quite plausible that the first-principles results are consistent with the observed[29] solvent shift in dilute solution of 0.33 ± 0.04 eV. Modern semiempirical simulations of the solvent shift of the liquid provide the same basic picture of the solvent shift as arising from both discrete inner-shell effects and long-range dielectric solvation,[32,34] but the relative importance of the two contributions is quite varied: Gao and Byan[32] predict larger contributions from specific solvation and a red shift for the dielectric component, whereas de Almeida et al.[34] predict only small specific solvation effects and very large dielectric solvation.

4. Conclusions

Strong hydrogen bonding with bonding energies of ca. 6 kcal mol^{-1} for the H_2O:pyrimidine complex, ca. 15 kcal mol^{-1} for asymmetric H_2O:H_2O:pyrimidine complexes, and ca. 11 kcal mol^{-1} for symmetric H_2O:pyrimidine:H_2O ones are predicted by the CCSD and B3LYP methods after basis set superposition error and zero-point corrections are included. Reasonable strong hydrogen bonds are also predicted for H_2O:pyrimidine and H_2O:H_2O:pyrimidine in their first (n,π^*) excited state, with the calculated bonding energies being 4.4−4.9 kcal mol^{-1} and 12.7 to 13.4 kcal mol^{-1}, respectively, but the two partial hydrogen bonds in H_2O:pyrimidine:H_2O are each quite weak with a combined bond strength of 6−7 kcal mol^{-1}.

The lowest energy hydrogen banded structures for both the ground and excited states are all planar structures with orthodox nitrogen or oxygen electron donors. Unorthodox structures in which hydrogen bonds form to the electron-rich π cloud of excited pyrimidine are also found but, whereas for H_2O:pyridine these above-ring structures are of considerably lower energy than those corresponding to the ground-state motif,[37] the orthodox hydrogen-bond structures are found to be the most stable ones for pyrimidine. This result is interpreted in terms of localization of the (n,π^*) excitation on the non-hydrogen-bonded nitrogen in the diazine complexes. It is clear that hydrogen bonding changes the fundamental nature of the excited-state electronic structure of pyrimidine and cannot be treated as a perturbation. Quite a different picture for excited-state hydrogen bonding is thus found from those depicted within other systems such as H_2O:formaldehyde[24] and H_2O:pyridine[37] and is suggestive that excited-state hydrogen bonding is vastly more complex than its well-known ground-state counterpart. In particular, we demonstrate that the electronic structure of the chromophore is determined by both the number and location of hydrogen-bonded water molecules.

For hydrogen bonding involving molecules in their ground states, it is rare that the hydrogen bonding induces dramatic changes in molecular electronic structure. A very important example, however, is the fine control exerted over primary

charge separation during photosynthesis by the protein environment.[89] This system involves a chlorophyll dimer cation radical known as the "special pair". Like the excited states of pyrimidine, the ground state of this system has a nearby electronic state and the primary chemical question concerns the localization or delocalization of the electrons over the system.[89,90] The study of diazines interacting with water thus provides a simple model system for an important complex biological phenomenon. Solvent interactions also control the electronic structure of symmetric mixed-valence inorganic complexes by a similar mechanism, forcing asymmetry in the electronic distribution.

Owing to the energy cost required to localize the (n,π^*) excitation and the fact that such localization is never complete,[91] the calculated hydrogen bond energies to pyrimidine in its excited $^1B_1$ (n,π^*) state are slightly less than those for the ground state. They remain substantially larger than those for H_2O:pyridine,[37] however, a system that is predicted to spontaneously dissociate following Franck−Condon excitation as the additional energy required to produce this excitation exceeds the weak excited-state bond strength. For H_2O:pyrimidine, however, the calculated predissociation energies E_{pre} are in excess of the 0−0 energy E_{00} by ca. 0.1 eV, increasing to 0.4 eV for the asymmetric doubly aquated species H_2O:H_2O:pyrimidine. This suggests that for these complexes bound excited-state complexes can be formed through tight control of the excitation energy. It is hence warranted that further efforts be made to observe these species in molecular beams.[8,9]

Baba, Goodman, and Valenti[4] concluded that in solution the hydrogen is broken in the excited state of pyridine and the azines. This view was based on the supposition that (n,π^*) excitation localizes on individual nitrogen atoms in the diazines, a view that has been subsequently shown to be incorrect for these molecules in the gas phase.[41,43,92] Quantitative simulations based on the assumption that the effects of hydrogen bonding could be treated merely as a perturbation to the delocalized-excitation gas-phase electronic structure[29] reproduced the key experimental results but quantitatively overestimated the magnitude of the observed solvent shifts by ca. 60%. Subsequently, Gao and Byun[32] used a semiclassical methodology to predict that (n,π^*) localization is induced by hydrogen bonding. As described above, our first principles calculations on small clusters verify their conclusions. Quantitatively, we conclude that it takes only 1−2 kcal mol^{-1} of energy to break the second hydrogen bond in the symmetric species H_2O:pyrimidine:H_2O; this quantity is small compared to possible alternate hydrogen-bond formation processes in solution, allowing liquid structure and entropy effects to break the hydrogen bond to the excited state, establishing more rigorously the original conclusions drawn by Baba, Goodman, and Valenti.[4] Excitation localization effects appear to reduce calculated solvent shifts by ca. one-third.

Acknowledgment. We thank the Australian Research Council for funding this research and Australian Partnership for Advanced Computing for the provision of computational resources.

Supporting Information Available: Analysis (pdf format) of the calculated and observed frequency changes on formation of both H_2O:pyrimidine, H_2O:pyrimidine:H_2O, and H_2O:H_2O:pyrimidine in their ground and excited electronic states, along with the calculated intermolecular vibration frequencies. All optimized structures, vibration frequencies, and normal modes for the complex and its constituents, as well as pertinent Duschinsky rotation matrices and geometry changes projected onto normal coordinates (ASCII format). This material is available free of charge via the Internet at http://pubs.acs.org.

References and Notes

(1) Rablen, P. R.; Lockman, J. W.; Jorgensen, W. L. *J. Phys. Chem. A* **1998**, *102*, 3782.
(2) Jeffrey, G. A.; Saenger, W. *Hydrogen Bonding in Biological Structure*; Springer-Verlag: Berlin, 1991.
(3) Baker, E. N.; Hubbard, R. E. *Prog. Biophys. Mol. Biol.* **1984**, *44*, 97.
(4) Baba, H.; Goodman, L.; Valenti, P. C. *J. Am. Chem. Soc.* **1966**, *88*, 5410.
(5) Mctigue, P.; Renowden, P. V. *J. Chem. Soc., Faraday I* **1975**, 1784.
(6) Carrabba, M. M.; Kenny, J. E.; Moomaw, W. R.; Cordes, J.; Denton, M. *J. Phys. Chem.* **1985**, *89*, 674.
(7) Schauer, M.; Bernstein, E. R. *J. Chem. Phys.* **1985**, *82*, 726.
(8) Wanna, J.; Menapace, J. A.; Bernstein, E. R. *J. Chem. Phys.* **1986**, *85*, 1795.
(9) Wanna, J.; Bernstein, E. R. *J. Chem. Phys.* **1987**, *86*, 6707.
(10) Maes, G.; Smets, J. *J. Mol. Struct.* **1992**, *270*, 141.
(11) Destexhe, A.; Smets, J.; Adamowicz, L.; Maes, G. *J. Phys. Chem.* **1994**, *98*, 1506.
(12) Zoidis, E.; Yarwood, J.; Danten, Y.; Besnard, M. *Mol. Phys.* **1995**, *85*, 373.
(13) Zoidis, E.; Yarwood, J.; Danten, Y.; Besnard, M. *Mol. Phys.* **1995**, *85*, 385.
(14) Buyl, F.; Smets, J.; Maes, G.; Adamowicz, L. *J. Phys. Chem.* **1995**, *99*, 14967.
(15) Del Bene, J. E.; Person, W.; Szczepaniak, K. *Mol. Phys.* **1996**, *89*, 47.
(16) Szczepaniak, K.; Chabrier, P.; Person, W. B.; Del Bene, J. E. *J. Mol. Struct.* **1997**, *436*−*437*, 367.
(17) Mccarthy, W.; Smets, J.; Adamowicz, L.; Plokhotzichenos, A. M.; Radchenko, E. D.; Shenia, G. G.; Stepanian, S. G. *Mol. Phys.* **1997**, *91*, 513.
(18) Zhang, B.; Cai, Y.; Mu, X.; Lou, N.; Wang, X. *J. Chem. Phys.* **2002**, *117*, 3701.
(19) Melandri, S.; Sanz, M. E.; Caminati, W.; Favero, P. G.; Kisiel, Z. *J. Am. Chem. Soc.* **1998**, *120*, 11504.
(20) Del Bene, J. E. *J. Am. Chem. Soc.* **1975**, *97*, 5330.
(21) Del Bene, J. E. *Chem. Phys.* **1976**, *15*, 463.
(22) Del Bene, J. E. *Chem. Phys.* **1980**, *50*, 1.
(23) Del Bene, J. E. *J. Phys. Chem.* **1994**, *98*, 5902.
(24) Del Bene, J. E.; Gwaltney, S. R.; Bartlett, R. J. *J. Phys. Chem. A* **1998**, *102*, 5124.
(25) Del Bene, J. E. *J. Comput. Chem.* **1981**, *2*, 422.
(26) Zeng, J.; Craw, J. S.; Hush, N. S.; Reimers, J. R. *Chem. Phys. Lett.* **1993**, *206*, 323.
(27) Zeng, J.; Craw, J. S.; Hush, N. S.; Reimers, J. R. *J. Chem. Phys.* **1993**, *99*, 1482.
(28) Zeng, J.; Hush, N. S.; Reimers, J. R. *J. Chem. Phys.* **1993**, *99*, 1495.
(29) Zeng, J.; Hush, N. S.; Reimers, J. R. *J. Chem. Phys.* **1993**, *99*, 1508.
(30) Zeng, J.; Hush, N. S.; Reimers, J. R. *J. Phys. Chem.* **1996**, *100*, 9561.
(31) Maes, G.; Smets, J.; Adamowicz, L.; McCarthy, W.; Van Bael, M. K.; L Houben; Shoone, K. *J. Mol. Struct.* **1997**, *410*−*411*, 315.
(32) Gao, J.; Byun, K. *Theor. Chim. Acta* **1997**, *96*, 151.
(33) Hush, N. S.; Reimers, J. R. *Chem. Rev.* **2000**, *100*, 775.
(34) de Almeida, K. J.; Coutinho, K.; de Almeida, W. B.; Rocha, W. R.; Canuto, S. *Phys. Chem. Chem. Phys.* **2001**, *3*, 1583.
(35) Martin, M. E.; Sanchez, M. L.; Aguilar, M. A.; del Valle, F. J. O. *J. Mol. Struct. (THEOCHEM)* **2001**, *537*, 213.
(36) Ramaekers, R.; Houben, L.; Adamowicz, L.; Maes, G. *Vibr. Spectrosc.* **2003**, *32*, 185.
(37) Cai, Z.-L.; Reimers, J. R. *J. Phys. Chem. A* **2002**, *106*, 8769.
(38) McRae, E. G. *J. Phys. Chem.* **1957**, *61*, 562.
(39) Liptay, W. In *Modern Quantum Chemistry*; Sinanoglu, O., Ed.; Academic Press: New York, 1965; Vol. III, p 45.
(40) Rettig, W. *J. Mol. Struct.* **1982**, *84*, 303.
(41) Zeng, J.; Woywod, C.; Hush, N. S.; Reimers, J. R. *J. Am. Chem. Soc.* **1995**, *117*, 8618.
(42) Kleier, D. A.; Martin, R. L.; Wadt, W. R.; Moomaw, W. R. *J. Am. Chem. Soc.* **1982**, *104*, 60.
(43) Fischer, G.; Cai, Z.-L.; Reimers, J. R.; Wormell, P. *J. Phys. Chem. A* **2003**, *107*, 3093.
(44) Karelson, M. M.; Zerner, M. C. *J. Am. Chem. Soc.* **1990**, *112*, 9405.
(45) Karelson, M. M.; Zerner, M. C. *J. Phys. Chem.* **1992**, *96*, 6949.
(46) Hush, N. S.; Reimers, J. R. *Coord. Chem. Rev.* **1998**, *177*, 37.
(47) Jorgensen, W. L.; McDonald, N. A. *J. Mol. Struct. THEOCHEM* **1988**, *424*, 145.

(48) Spoliti, M.; Bencivenni, L.; Ramondo, F. *THEOCHEM* **1994**, *303*, 185.
(49) Smets, J.; Adamowicz, L.; Maes, G. *J. Mol. Struct.* **1994**, *322*, 113.
(50) Martoprawiro, M. A.; Bacskay, G. B. *Mol. Phys.* **1995**, *85*, 573.
(51) Samanta, U.; Chakrabarti, P.; Chandrasekhar, J. *J. Phys. Chem. A* **1998**, *102*, 8964.
(52) Smets, J.; McCarthy, W.; Maes, G.; Adamowicz, L. *J. Mol. Struct.* **1999**, *476*, 27.
(53) Dkhissi, A.; Adamowicz, L.; Maes, G. *J. Phys. Chem.* **2000**, *104*, 2112.
(54) Papai, I.; Jancso, G. *J. Phys. Chem.* **2000**, *104*, 2132.
(55) Bauernschmitt, R.; Ahlrichs, R. *Chem. Phys. Lett.* **1996**, *256*, 454.
(56) Bauernschmitt, R.; Häser, M.; Treutler, O.; Ahlrichs, R. *Chem. Phys. Lett.* **1997**, *264*, 573.
(57) Casida, M. E.; Jamorski, C.; Casida, C. K.; Salahub, D. R. *J. Chem. Phys.* **1998**, *108*, 4439.
(58) Stratmann, R. E.; Scuseria, G. E.; Frisch, M. J. *J. Chem. Phys.* **1998**, *109*, 8218.
(59) van Gisbergen, S. J. A.; Kootstra, F.; Schipper, P. R. T.; Gritsenko, O. V.; Snijders, J. G.; Baerends, E. J. *Phys. Rev. A* **1998**, *57*, 2556.
(60) Tozer, D. J.; Amos, R. D.; Handy, N. C.; Roos, B. O.; Serrano-Andrés, L. *Mol. Phys.* **1999**, *97*, 859.
(61) Becke, A. D. *J. Chem. Phys.* **1993**, *98*, 5648.
(62) Becke, A. D. *Phys. Rev. A* **1988**, *38*, 3098.
(63) Lee, C.; Yang, W.; Parr, R. G. *Phys. Rev. B* **1988**, *37*, 785.
(64) Hegarty, D.; Robb, M. A. *Mol. Phys.* **1979**, *38*, 1795.
(65) Andersson, K.; Malmqvist, P.-C.; Roos, B. O. *J. Chem. Phys.* **1992**, *96*, 1218.
(66) Purvis III, G. D.; Bartlett, R. J. *J. Chem. Phys.* **1982**, *76*, 1910.
(67) Stanton, J. F.; Bartlett, R. J. *J. Chem. Phys.* **1993**, *98*, 7029.
(68) Ahlrichs, R.; Bär, M.; Baron, H.-P.; Bauernschmitt, R.; Böcker, S.; Ehrig, M.; Eichkorn, K.; Elliot, S.; Haase, F.; Häser, M.; Horn, H.; Huber, C.; Huniar, U.; Kattannek, M.; Kölmel, C.; Kollwitz, M.; Ochsenfeld, C.; Öhm, H.; Schäfer, A.; Schneider, U.; Treutler, O.; von Arnim, M.; Weigend, F.; Weis, P.; Weiss, H. *TURBOMOLE*; Quantum Chemistry Group The University of Karlsure: Karlsruhe, 1997 Version 4.
(69) Eichkorn, K.; Treutler, O.; Oehm, H.; Haeser, M.; Ahlrichs, R. *Chem. Phys. Lett.* **1995**, *242*, 652.
(70) *CPMD (Car-Parrinello Molecular Dynamics)*; IBM Corp. and MPI fuer Festkoerprtforschung: Stuttgart, 1997−2001.
(71) Frisch, M. J.; Trucks, G. W.; Schlegel, H. B.; Scuseria, G. E.; Robb, M. A.; Cheeseman, J. R.; Zakrzewski, V. G.; Montgomery, J. A.; Stratmann, R. E.; Burant, J. C.; Dapprich, S.; Millam, J. M.; Daniels, A. D.; Kudin, K. N.; Strain, M. C.; Farkas, O.; Tomasi, J.; Barone, V.; Cossi, M.; Cammi, R.; Mennuci, B.; Pomelli, C.; Adamo, C.; Clifford, S.; Ochtersi, J.; Patterson, G. A.; Ayala, P. Y.; Cui, Q.; Morokuma, K.; Malick, D. K.; Rabuck, A. D.; Raghavachari, K.; Foresman, J. B.; Cioslowski, J.; Ortiz, J. V.; Stefanov, B. B.; Liu, G.; Liashenko, A.; Piskorz, P.; Komaromi, I.; Gomperts, R.; Martin, R. L.; Fox, D. J.; Keith, T.; Al-Laham, M. A.; Peng, C. Y.; Nanayakkara, A.; Gonzalez, G.; Challacombe, M.; Gill, P. M. W.; Johnson, B. G.; Wong, W. Chen.; Wong, M. W.; Andres, J. L.; Head-Gordon, M.; Replogle, E. S.; Pople, J. A. *Gaussian 98*, revision A7; Gaussian Inc.: Pittsburgh, PA, 1998.
(72) Stanton, J. F.; Gauss, J.; Watts, J. D.; Nooijen, M.; Oliphant, N.; Perera, S. A.; Szalay, P. G.; Lauderdale, W. J.; Gwaltney, S. R.; Beck, S.; Balková, A.; Bernholdt, D. E.; Baeck, K.-K.; Rozyczko, P.; Sekino, H.; Hober, C.; Bartlett, R. J. *ACES II*; Quantum Theory Project The University of Florida: Gainsville, 1999.
(73) Helgaker, T.; Jensen, H. J. Aa.; Joergensen, P.; Olsen, J.; Ruud, K.; Aagren, H.; Andersen, T.; Bak, K. L.; Bakken, V.; Christiansen, O.; Dahle, P.; Dalskov, E. K.; Enevoldsen, T.; Fernandez, B.; Heiberg, H.; Hettema, H.; Jonsson, D.; Kirpekar, S.; Kobayashi, R.; Koch, H.; Mikkelsen, K. V.; Norman, P.; Packer, M. J.; Saue, T.; Taylor, P. R.; Vahtras, O. *Dalton* release 1.0, 1997.
(74) Andersson, K.; Blomberg, M. R. A.; Fülscher, M. P.; Karlström, G.; Lindh, R.; Malmqvist, P.-C.; Neogrády, P.; Olsen, J.; Roos, B. O.; Sadlej, A. J.; Seijo, L.; Serrano-Andrés, L.; Siegbahn, P. E. M.; Widmark, P.-O. *Molcas Version 4*; University of Lund: Lund, 1997.
(75) Werner, H.-J.; Knowles, P. J.; Amos, R. D.; Bernhardsson, A.; Berning, A.; Celani, P.; Cooper, D. L.; Deegan, M. J. O.; Hampel, C.; Lindh, R.; Lloyd, A. W.; Meyer, W.; Nicklass, A.; Peterson, K.; Pitzer, R.; Stone, A. J.; Taylor, P. R.; Mura, M. E.; Pulay, P.; Schütz, M.; Stoll, H.; Thorsteinsson, T. *MOLPRO-2000*; University of Birmingham: Birmingham, U.K., 2000.
(76) Foresman, J. B.; Head-Gordon, M.; Pople, J. A.; Frisch, M. J. *J. Phys. Chem.* **1992**, *96*, 135.
(77) Hehre, W. J.; Ditchfield, R.; Pople, J. A. *J. Chem. Phys.* **1972**, *56*, 2257.
(78) Kendall, R. A.; Dunning Jr, T. H.; Harrison, R. J. *J. Chem. Phys.* **1992**, *96*, 6796.
(79) Dunning Jr, T. H. *J. Chem. Phys.* **1989**, *90*, 1007.
(80) Scott, A. P.; Radom, L. *J. Phys. Chem.* **1996**, *100*, 16502.
(81) Boys, S. F.; Benardi, F. *Mol. Phys.* **1970**, *19*, 553.
(82) van Duijneveldt, F. B.; van Duijnevldt-van de Rijdt, G. C.; van Leuthe, J. H. *Chem. Rev.* **1994**, *94*, 1973.
(83) Dunning, T. H., Jr. *J. Phys. Chem. A* **2000**, *104*, 9062.
(84) Lambropoulos, N. A.; Reimers, J. R.; Hush, N. S. *J. Chem. Phys.* **2002**, *116*, 10277.
(85) Innes, K. K.; Ross, I. G.; Moomaw, W. R. *J. Mol. Spectrosc.* **1988**, *132*, 492.
(86) Hoy, A. R.; Bunker, P. B. *J. Mol. Spectrosc.* **1974**, *74*, 1.
(87) Herzberg, G. *Molecular spectra and molecular structure. III. Electronic spectra and electronic structure of polyatomic molecules*; D. Van Nostrand: Princeton, NJ, 1966.
(88) Kim, J. H.; Lee, H.-J.; Kim, E.-J.; Jung, H. J.; Choi, Y.-S.; Park, J.; Yoon, C.-J. *J. Phys. Chem. A* **2004**, *108*, 921.
(89) Reimers, J. R.; Hush, N. S. *J. Am. Chem. Soc.* **2004**, *126*, 4132.
(90) Reimers, J. R.; Hush, N. S. *J. Chem. Phys.* **2003**, *119*, 3262.
(91) Reimers, J. R.; Hush, N. S. *Chem. Phys.* **1993**, *176*, 407.
(92) Weber, P.; Reimers, J. R. *J. Phys. Chem. A* **1999**, *103*, 9830.
(93) Bolovinos, A.; Tsekeris, P.; Philis, J.; Phantos, E.; Andritsopoulos, G. *J. Mol. Spectrosc.* **1984**, *103*, 240.